33p

SECURITY INFORMATION

[redacted]

Copy 408
RM E52C13

NACA RM E52C13

N63-14759
Code-1

NACA CLASSIFICATION CHANGED TO DECLASSIFIED EFFECTIVE 12 MARCH 63 AUTHORITY NASA CCN 3 BY J.J.CARROLL

RESEARCH MEMORANDUM

EMPIRICAL COOLING CORRELATION FOR AN EXPERIMENTAL AFTERBURNER WITH AN ANNULAR COOLING PASSAGE

By William K. Koffel and Harold R. Kaufman

Lewis Flight Propulsion Laboratory
Cleveland, Ohio

OTS PRICE

XEROX $ 3.60 pd

MICROFILM $ 1.19 my

CLASSIFIED DOCUMENT

This material contains information affecting the National Defense of the United States within the meaning of the espionage laws, Title 18, U.S.C., Secs. 793 and 794, the transmission or revelation of which in any manner to an unauthorized person is prohibited by law.

NATIONAL ADVISORY COMMITTEE
FOR AERONAUTICS

WASHINGTON
June 26, 1952

[redacted]

DECLASSIFIED

[redacted]

NATIONAL ADVISORY COMMITTEE FOR AERONAUTICS

RESEARCH MEMORANDUM

EMPIRICAL COOLING CORRELATION FOR AN EXPERIMENTAL AFTERBURNER WITH AN ANNULAR COOLING PASSAGE

By William K. Koffel and Harold R. Kaufman

SUMMARY

14759

An empirical cooling correlation is established for an experimental high-performance afterburner. This correlation relates the average combustion-chamber wall temperature at a station near the combustion-chamber outlet to the temperatures of the cooling air and combustion gas, and to the mass flows of the cooling air and combustion gas. The correlation equation is a useful device for shortening the experimental investigation of afterburner cooling characteristics inasmuch as it provides a method for interpolating, or to a limited extent extrapolating, the critical wall temperatures for other combinations of the operating variables than those tested.

For the experimental afterburner investigated, the circumferential average wall temperature could be correlated with a spread from the experimental data of $\pm 50^{\circ}$ R over a range of combustion-gas bulk temperature from 1810° to 3500° R.

The achievement of high performance and good operational characteristics simultaneously in an afterburner over a wide range of operating conditions requires certain arrangements of fuel distribution and flameholder geometry. Inasmuch as the latitude of these arrangements is relatively small, the results for this afterburner are believed representative of most high-performance afterburners.

Two other radial distributions of afterburner fuel across the turbine-outlet annulus were investigated and are discussed.

INTRODUCTION

Operational gas temperatures in both current and projected afterburners are such that some form of cooling system is required to maintain safe wall temperatures. One widely used form of cooling is provided by air flowing through an annular passage surrounding the combustion chamber. Design calculations of this system based on previously available heat-transfer data are, however, questionable because of the widely different

[redacted]

[redacted]

flow conditions between afterburners and conventional heat-transfer setups and because of other unverified assumptions. Accordingly, a carefully instrumented and controlled experimental afterburner was built by the Lewis laboratory of the NACA to study the cooling characteristics and temperature profiles in an actual afterburner cooled by air flowing through an annular cooling passage. This installation also provided data on the heat-transfer process between the combustion gases and the walls, and data for examining the possibility of establishing an empirical cooling correlation to provide a convenient and rapid method for calculating the wall temperatures from commonly known performance parameters. In reference 1 the effects of afterburner fuel-air ratio (exhaust-gas temperatures from approximately 3060° to 3825° R), radial distribution of afterburner fuel flow, and combustion gas flow on the temperature profiles of the combustion gas and on the temperature profiles of the combustion-chamber walls are tabulated and graphically presented. The variations of wall temperatures with the mass-flow ratio of cooling-air to combustion-gas flow and with inlet cooling-air temperature were also determined. An analysis of the heat-transfer process in the combustion chamber is given in reference 2 along with the effect of three radial distributions of afterburner fuel on the convective heat-transfer coefficient for the combustion gas.

This report deals with the final objective. The form of a cooling correlation equation is analytically derived and the experimental data of this investigation are used to empirically evaluate the constants in the equation. The resulting equation correlates the circumferential average wall temperature at a station near the combustion-chamber exit with the bulk temperatures of the combustion gas and cooling air at that station and with the mass-flow ratio of cooling air to combustion gas. Because design information is often given in terms of the usual engine performance parameters, methods are developed for relating the temperatures in the correlation equation to the usually known temperatures at the burner inlet (turbine outlet), at the exhaust-nozzle exit, and at the cooling-passage inlet, and to the mass flows of cooling air and combustion gas.

The empirical constants in the correlation equation may vary with burner design; however, the performance and operating characteristics of the afterburner tested were very good so that the cooling correlation for other high-performance afterburners would probably be similar. More experience is required before it can be determined just how much these constants may vary among high-performance afterburners. Meanwhile, the use of the empirical correlation for this afterburner can provide a method of shortening the experimental investigation of cooling for other afterburners by providing a means of interpolating or extrapolating the wall-temperature data to conditions other than those tested.

[redacted]

DECLASSIFIED

SYMBOLS

The following symbols are used in this report:

$B = \frac{3600\ W_a c_{p,a}}{U\pi Dg}$	(ft)
C	numerical constant or an arbitrary constant
c_p	specific heat at constant pressure (Btu/(lb)(^oR))
D	diameter (ft)
D_h	hydraulic diameter of cooling passage (ft)
f	correction factor, $f = T_{a,F}/(T_{a,F})_{0.12}$
G	mass velocity (lb/(sec)(sq ft))
h	heat-transfer coefficient (Btu/(hr)(sq ft)(^oR))
K	empirical constant
k	thermal conductivity (Btu/(hr)(ft)(^oR))
L	distance from flame-holder center line to exhaust-nozzle exit (ft)
m,n, and p	exponents
T	bulk total temperature or surface temperature (^oR)
U	over-all heat-transfer coefficient (Btu/(hr)(sq ft)(^oR))
W	gas flow (lb/sec)
x	distance downstream of flame-holder center line (ft)
θ	$T_g - T_a$, ^oR
μ	absolute viscosity (lb/(ft)(sec))

Subscripts:

a	cooling air
B,C,D,E,F,G	stations along the combustion-chamber length
e	effective

[redacted]

03912A1030

g	gas or combustion chamber
w	combustion-chamber wall
x	variable station
0	flame-holder center line
0.12	corresponding to mass-flow ratio of 0.12
1	exhaust-nozzle exit
2	and higher are used to distinguish between specific constants

APPARATUS AND PROCEDURE

Test Installation

A schematic drawing of the experimental afterburner used in this cooling investigation is shown in figure 1. The cylindrical combustion chamber had a length of 5 feet from the flame-holder center line to the exhaust-nozzle inlet and an inside diameter of 26 inches; the annular cooling passage had a height of 1/2 inch. The flame holder had a single V-gutter with sinusoidal corrugations on the trailing edges. The V-gutter had a mean diameter of 18 inches, a mean width across the corrugations of $1\frac{3}{4}$ inches, and an included angle of 35°. The blockage at the downstream face of the flame holder was about 23 percent, and the velocity at the flame holder under the conditions of the investigation was approximately 480 feet per second.

Twelve radial, fuel spray bars were equally spaced circumferentially in a plane 8.75 inches downstream of the turbine flange and 13.25 inches upstream of the flame-holder center line. Three different configurations (12 spray bars per configuration) of spray bars were used to study the effects of various radial fuel distributions on empirical constants in the cooling correlation equation. Configuration A (fig. 2) produced a nearly uniform fuel distribution. Configuration B increased the fuel concentration near the combustion-chamber wall and decreased the fuel flow in the center of the combustion chamber. Configuration C concentrated more fuel at the center and decreased the concentration near the combustion-chamber walls.

Instrumentation

Extensive instrumentation was provided at six longitudinal stations (fig. 1), B, C, D, E, F, and G, with four of these stations, C, D, E, and F, having six circumferential groups of instrumentation. (The instrumentation is described in detail in reference 1.)

[redacted]

DECLASSIFIED

Because of the large number of thermocouples, four flight recorders were used to reduce the recording time while maintaining equilibrium conditions. The estimated over-all accuracy of the individual temperature measurements are as follows:

Wall temperature, $^{\circ}F$	± 15
Cooling air, $^{\circ}F$	± 10
Exhaust-gas temperature, $^{\circ}F$	± 50

The temperatures of the combustion-chamber wall and of the cooling air in this report are arithmetic averages of their respective temperatures measured at six equally spaced positions around the circumference of the burner.

Range of Test Data

The afterburner in this investigation incorporated the best available experimental design information for high performance. Preliminary tests were conducted on a similar uninstrumented afterburner to confirm that the afterburner configuration for this investigation had high performance and good operating characteristics over a wide range of fuel-air ratio and altitude. The final geometry of the turbine diffuser inner cone and flame holder in combination with the fuel spray bars producing approximately uniform distribution of fuel across the turbine annulus is designated configuration A. The various combinations of conditions and afterburner configurations investigated are tabulated in the following table:

[redacted]

[redacted]

Configuration	Altitude (ft)	Exhaust-gas temperature $T_{g,1}$ (°R)	Combustion-gas flow W_g (lb/sec)	Mass-flow ratio W_a/W_g	Cooling-air inlet temperature $T_{a,0}$ (°R)
A	30,000	3060	22.1	0.0672 to .1872	500 to 1587
	30,000	3240	22.2	0.1002 to .1917	500 to 1222
	30,000	3435	22.3	0.0953 to .1796	502 to 1408
	40,000	3265	13.8	0.1440	528 to 1340
	30,000	3825	22.8	0.1374 to .1906	515
B	30,000	3215	22.2	0.0985 to .1891	495 to 1223
C	30,000	3235	22.3	0.1420	524 to 1450
	30,000	3764	22.4	0.1912	524

Configurations A, B, and C differ only in the radial distribution of fuel across the turbine-outlet annulus. Because of the negligible heat transfer to the cooling air just upstream of station B, the inlet cooling-air temperature $T_{a,0}$ was taken equal to the cooling-air temperature measured at station B. The mass-flow rate of cooling air W_a and the inlet cooling-air temperature $T_{a,0}$ were systematically and independently varied while holding all other quantities constant. All data are for a simulated flight Mach number of 0.52 and rated engine speed. Most of the data were obtained by adjusting the afterburner fuel flow in order to maintain an average burner inlet (turbine outlet) temperature of 1633 $\pm$ 12° R, which resulted in a nearly constant gas temperature at the exhaust-nozzle exit for a given exit area.

ANALYSIS

Derivation of Cooling Correlation Equation

The form of the cooling correlation equation is developed in the following paragraphs from a heat balance across the combustion-chamber

[redacted]

DECLASSIFIED

wall at station x (fig. 3) on the assumption that there are no external heat losses and that heat is transferred by forced convection only. The assumption is valid since the outside wall of the cooling passage was insulated. About one fourth of the heat was transferred to the combustion-chamber wall by nonluminous radiation (reference 2), but it is convenient to derive the form of the correlation equation by neglecting radiation and to assume that radiation and other unknown effects can be accounted for by the empirical evaluation of constants appearing in the equation.

The heat balance at station x can be written as

$$h_{g,x}(T_{g,x} - T_{w,x}) = h_{a,x}(T_{w,x} - T_{a,x}) \tag{1}$$

or

$$\frac{T_{g,x} - T_{w,x}}{T_{w,x} - T_{a,x}} = \frac{h_{a,x}}{h_{g,x}} \tag{2}$$

The convective heat-transfer coefficient for turbulent flow of gases is given approximately by (reference 3)

$$\frac{hD}{k} = C_2 \left(\frac{GD}{\mu}\right)^m \tag{3}$$

An approximate relation between viscosity and temperature is (reference 4)

$$\frac{\mu}{\mu_0} = \left(\frac{T}{T_0}\right)^n \tag{4}$$

and the viscosity and thermal conductivity are related approximately by

$$k = C_3\mu \tag{5}$$

Substituting equations (4) and (5) into equation (3) and rearranging give

$$h = C_4\mu_0^{1-m} \left(\frac{T}{T_0}\right)^{n(1-m)} \frac{G^m}{D^{1-m}} \tag{6}$$

[redacted]

CONFIDENTIAL

The substitution of equation (6) into equation (2) and the application of the subscripts a and g for air and gas, respectively, give

$$\frac{T_{g,x} - T_{w,x}}{T_{w,x} - T_{a,x}} = C_5 \frac{\mu_{a,0}^{1-m} \left(\frac{T_{a,x}}{T_{a,0}}\right)^{n(1-m)} G_a^{m} D_g^{1-m}}{\mu_{g,0}^{1-m} \left(\frac{T_{g,x}}{T_{g,0}}\right)^{n(1-m)} G_g^{m} D_{h,a}^{1-m}} \tag{7}$$

but

$$\frac{\mu_{a,0}}{\mu_{g,0}} = \left(\frac{T_{a,0}}{T_{g,0}}\right)^{n} \tag{8}$$

because the viscosity of the combustion gas and of the cooling air can be practically represented by the same curve. Substituting equation (8) into equation (7) and simplifying give

$$\frac{T_{g,x} - T_{w,x}}{T_{w,x} - T_{a,x}} = C_6 \left(\frac{T_{a,x}}{T_{g,x}}\right)^{n(1-m)} \left(\frac{G_a}{G_g}\right)^{m} \left(\frac{D_g}{D_{h,a}}\right)^{1-m} \tag{9}$$

Equation (9) reduces to

$$\frac{T_{g,x} - T_{w,x}}{T_{w,x} - T_{a,x}} = K \left(\frac{T_{a,x}}{T_{g,x}}\right)^{p} \left(\frac{W_a}{W_g}\right)^{m} \tag{10}$$

for a constant geometry. Inasmuch as radiation was neglected and approximate expressions were used in this derivation, it is to be expected that the exponents p and m will not be uniquely related as are the exponents in equation (9).

Equation (10) states that the parameter $\frac{T_{g,x} - T_{w,x}}{T_{w,x} - T_{a,x}}$ will plot as a straight line, on log-log coordinates, against either the ratio $T_{a,x}/T_{g,x}$ or W_a/W_g when the remaining ratio is held fixed. Thus the exponents p and m can be evaluated empirically if the experimental data plot as straight lines on log-log coordinates. The constant and the exponents in equation (10) will be determined later for the average wall temperature at station F, 4 feet downstream of the flame holder and 1 foot upstream of the nozzle inlet. Station G was closer to the exhaust nozzle inlet, but station F was used because the instrumentation was more complete than at station G. The wall temperatures at station G are about 100° to 150° R hotter than at station F for $T_{g,F}$ of 2850° and 3170° R, respectively (reference 1).

[redacted]

DECLASSIFIED

Relation of $T_{g,x}$ and $T_{a,x}$ to Known Parameters

The wall temperature $T_{w,x}$ at station x is given in equation (10) as a function of the corresponding bulk total temperatures of the combustion gas $T_{g,x}$, and the cooling air $T_{a,x}$, and of the flow rates of the cooling air W_a and combustion gas W_g. However, a designer may be given only the total temperatures at the burner inlet $T_{g,0}$ and at the exhaust nozzle outlet $T_{g,1}$, the inlet cooling-air total temperature $T_{a,0}$, and the flow rates W_a and W_g from afterburner performance data. It is therefore necessary to relate $T_{g,x}$ to $T_{g,0}$ and $T_{g,1}$ and to relate $T_{a,x}$ to the temperatures $T_{g,0}$, $T_{g,1}$, $T_{a,0}$, and to the flow rates W_a and W_g.

The value of $T_{g,x}$ was not measured directly in this investigation so that it was necessary to obtain an equation for the longitudinal distribution of the combustion-gas total temperature. It has been found that the calculated longitudinal distribution (see method of reference 5) of the total temperature in ram-jet combustion chambers, having internal geometries and fuel systems somewhat similar to the afterburner of this investigation, are generalized quite well (fig. 4) by the equation

$$\frac{T_{g,x} - T_{g,0}}{T_{g,1} - T_{g,0}} = \sin \frac{\pi}{2} \frac{x}{L} \tag{11}$$

As a check on the applicability of equation (11) to the afterburner of this investigation, the longitudinal distribution of static pressure was calculated by the principles in reference 5 from the temperature distribution of equation (11). The agreement between the calculated curves (fig. 5) and the symbols representing the experimental pressure distribution is very good. In view of this agreement and of the results of figure 4, equation (11) was used to calculate $T_{g,x}$ in this report. Equation (11) states that the rise in combustion-gas temperature to station F ($x/L = 0.651$) is 0.85 of the temperature rise from the flame holder to the exhaust-nozzle exit.

Equation and design charts are developed in appendix A for the purpose of calculating the temperature $T_{a,x}$ for any combination of the independent design variables $T_{g,0}$, $T_{g,1}$, $T_{a,0}$, W_a, and W_g. These charts are convenient for design calculations, and the development illustrates a procedure for interpolating the values of $T_{a,x}$ measured in other afterburners. Use of the charts in the correlation equation for calculating the wall temperature at station F is illustrated in the sample problem of appendix C.

[redacted]

RESULTS AND DISCUSSION

Determination of Cooling Correlation Constants

The exponent p was determined from figure 6(a). The data of several series for which the mass-flow ratio was constant fall approximately along a straight line having a slope of 0.73. The exponent m was found from the slope of figure 6(b) to equal 0.80 for several series of data in which both the temperature ratio $T_{a,F}/T_{g,F}$ and the mass-flow ratio W_a/W_g were varied. The constant K equals 30, corresponding to the intercept of the parameter $\frac{T_{g,F} - T_{w,F}}{T_{w,F} - T_{a,F}}\left(\frac{T_{a,F}}{T_{g,F}}\right)^{-0.73}$ at a mass-flow ratio of unity. The working correlation equation for configuration A is then

$$\frac{T_{g,F} - T_{w,F}}{T_{w,F} - T_{a,F}} = 30\left(\frac{T_{a,F}}{T_{g,F}}\right)^{0.73}\left(\frac{W_a}{W_g}\right)^{0.80} \tag{12}$$

The exponent of the mass-flow ratio agrees with the handbook values for turbulent convection. The exponent of the temperature ratio $T_{a,F}/T_{g,F}$ is about two and one half times the value of 0.3, corresponding to turbulent convention alone (see reference 6). This difference is attributed to radiation.

The data from configurations B and C, in which the radial distribution of afterburner fuel was varied, were correlated by similar plots (fig. 7) giving different constants and somewhat different exponents. The correlations for configurations B and C are not applicable to good afterburners because these configurations had poor performance and undesirable operating or cooling characteristics (reference 1), but they do illustrate how much the wall temperature can be affected. The wall temperatures calculated from the respective correlation for each configuration are shown to better advantage in figure 8 for a combustion-gas temperature $T_{g,F}$ of 3500° R and a mass-flow ratio of 0.143. The wall temperature at station F increases approximately linearly for all three configurations as the cooling-air temperature increases from 800° R (corresponding to an inlet cooling-air temperature $T_{a,0}$ of about 500° R). The wall temperature resulting from configuration B was about 180° hotter than for configuration A, whereas the wall temperature for configuration C was 50° colder than for configuration A. The simultaneous achievement of high performance and good operational characteristics over a wide range of operating conditions in an afterburner requires certain arrangements of fuel distribution and flameholder geometry. Inasmuch as the latitude of these arrangements is relatively small, the results for configuration A are believed representative of most high-performance afterburners, whereas configurations B and C are not representative.

[redacted]

DECLASSIFIED

Comparison of Wall Temperatures from Correlation

with Experimental Wall Temperatures

The quality of the correlation cannot be determined very well from figure 6(b). The agreement between the wall temperature from the correlation and the corresponding experimental wall temperature is dependent on the scatter in the data points used for evaluating the empirical constants and whether the correlation accounts for the effects of all significant variables. An indication of the degree to which this was achieved is shown by the agreement between the calculated average wall temperature and the corresponding average experimental wall temperature. Figure 9(a) shows that an agreement of $\pm 50^{\circ}$ R or less was obtained for the large number of data points for configuration A over a range of $T_{g,F}$ from about 1810° to 3500° R and for burner inlet temperatures of about 1342° to 1633° R. The same agreement resulted for data with a burner inlet temperature of 1633° R when the calculated values of $T_{a,F}$ from the working charts of appendix A were used in the correlation equation for configuration A (fig. 9(b)).

CONCLUDING REMARKS

An empirical cooling correlation is established for an experimental high-performance afterburner. The correlation equation is a means of shortening the experimental investigation of the afterburner cooling characteristics by providing a means of interpolating, or to a limited extent extrapolating, the critical wall temperatures for other combinations of the operating variables than those tested.

The data for the empirical cooling correlation developed in this report were obtained from an experimental afterburner cooled by air flowing through an annular cooling passage 1/2 inch in height. The cylindrical combustion chamber had an inside diameter of 26 inches and a length of 5 feet from flame holders to exhaust-nozzle inlet.

The average wall temperatures calculated from the correlation equation agreed within $\pm 50^{\circ}$ R of the corresponding average experimental temperatures at a station where the combustion gas had achieved 0.85 of the temperature rise from the flame holder to the exhaust-nozzle exit. The correlation yielded calculated wall temperatures within this agreement for combustion-gas temperatures at this station ranging from about 1810° to 3500° R.

Three radial distributions of afterburner fuel across the turbine outlet annulus were investigated. Similar correlations for wall temperature were obtained for each fuel distribution but with somewhat different empirical constants. One fuel distribution resulted in wall temperatures 180° R higher and another in wall temperatures 50° R lower than the best fuel distribution investigated; but these temperature variations were accompanied by poor performance and undesirable operating or cooling characteristics. The simultaneous achievement of high

03912A1030

performance and good operational characteristics over a wide range of operating conditions in an afterburner requires certain arrangements of fuel distribution and flame-holder geometry. Inasmuch as the latitude of these arrangements is relatively small, the results for the configuration with the best fuel distribution are believed representative of most high-performance afterburners, whereas the correlations for the other fuel distributions are not representative.

Lewis Flight Propulsion Laboratory
National Advisory Committee for Aeronautics
Cleveland, Ohio

[redacted]

DECLASSIFIED

APPENDIX A

RELATION OF $T_{a,F}$ TO DESIGN VARIABLES

The form of the function relating $T_{a,F}$ to the design variables is first obtained for a heat exchanger (fig. 3) representing the combustion chamber and the cooling-air passage and then modified to fit the experimental data. The characteristic equation for this heat exchanger is (derivation in appendix B)

$$\frac{T_{g,x} - T_{a,x}}{T_{g,1} - T_{g,0}} = \left(\frac{T_{g,0} - T_{a,0}}{T_{g,1} - T_{g,0}} - \frac{2\pi LB}{(\pi B)^2 + 4L^2}\right) e^{-\frac{x}{B}} + \frac{2\pi LB}{(\pi B)^2 + 4L^2} \cos \frac{\pi}{2} \frac{x}{L} + \frac{(\pi B)^2}{(\pi B)^2 + 4L^2} \sin \frac{\pi}{2} \frac{x}{L} \tag{A1}$$

where

$$B = \frac{3600\ W_a c_{p,a}}{U\pi D_g} \tag{A2}$$

Figure 10 is a plot of equation (A1) for $x/L = 0.651$ (station F). Equation (A1) was derived on the basis that the over-all heat-transfer coefficient U between the combustion gas and the cooling air is independent of x. However, U varies with x in an actual afterburner (reference 2) so that it is necessary to determine an effective value of U that is constant over the distance x. This constant value U_e has been evaluated for the range of the experimental data for x equal to the distance from the flame holder to station F. The values of U_e would have been different if another station had been chosen. The determination of U_e constitutes the fitting of equation (A1) to the afterburner tested. This fitting was accomplished for station F by substituting the calculated value of $T_{g,F}$ and the measured values of $T_{g,1}$, $T_{g,0}$, $T_{a,F}$, and $T_{a,0}$ into equation (A1) or more simply into the parameters of figure 10 and obtaining the value of B. With this value of B and the measured value of W_a, equation (A2) was solved for U_e.

The values of U_e to be used in calculating $T_{a,F}$ were plotted in figure 11(a) against the inlet cooling-air temperature $T_{a,0}$ for several exhaust-gas temperatures $T_{g,1}$ with a burner inlet temperature $T_{g,0}$ of 1633° R and a mass-flow ratio of 0.144. The effect of exhaust-gas temperature level on U_e is of the same order as the scatter so

03T412AJ039

that a mean line was drawn through the data. The values of U_e for a mass-flow ratio of 0.098 are shown in figure 11(b). Values of U_e for other mass-flow ratios can be read from figure 12, which is a cross plot of figures 11(a) and 11(b). It was found that for an inlet cooling-air temperature $T_{a,0}$ of 500° R, U_e was practically a linear function of the mass-flow ratio when plotted on log-log coordinates. Straight lines were drawn through the cross-plotted values of U_e (from figs. 11(a) and 11(b)) for other values of $T_{a,0}$.

Simple working charts relating $T_{a,F}$ to the generally known temperatures $T_{g,0}$, $T_{g,1}$, $T_{a,0}$ and mass-flow ratio were developed from equations (11), (A1), and (A2) from the values of U_e from figure 12. The first chart (fig. 13) shows the calculated cooling-air temperature $T_{a,F}$ plotted against the inlet cooling-air temperature for a mass-flow ratio of 0.12. The value of $T_{a,F}$ at any other mass-flow ratio is obtained by multiplying $T_{a,F}$ at $W_a/W_g = 0.12$ by the factor f from the second chart (fig. 14) corresponding to the particular values of $T_{a,0}$ and W_a/W_g.

[redacted]

DECLASSIFIED

APPENDIX B

DERIVATION OF LONGITUDINAL DISTRIBUTION OF COOLING-AIR TEMPERATURE

The one-dimensional distribution of cooling-air temperature is derived by assuming that the over-all heat-transfer coefficient U is independent of the distance downstream of the flame holder. It is also assumed that the longitudinal distribution of the combustion-gas total temperature is given by the equation

$$\frac{T_{g,x} - T_{g,0}}{T_{g,l} - T_{g,0}} = \sin \frac{\pi}{2} \frac{x}{L} \tag{B1}$$

Differentiation of equation (B1) and consideration of $T_{g,0}$ and $T_{g,l}$ as constants give

$$\frac{dT_{g,x}}{dx} = \frac{\pi}{2L} (T_{g,l} - T_{g,0}) \cos \frac{\pi}{2} \frac{x}{L} \tag{B2}$$

The heat balance at station x is

$$U\pi D_g(T_g - T_a)\, dx = 3600\, W_a c_{p,a} dT_a \tag{B3}$$

or

$$\frac{dT_a}{dx} = \frac{T_g - T_a}{\frac{3600\, W_a c_{p,a}}{U\pi D_g}} \equiv \frac{\theta}{B} \tag{B4}$$

where

$$\theta = T_g - T_a \tag{B5}$$

and

$$B = \frac{3600\, W_a c_{p,a}}{U\pi D_g} \tag{B6}$$

Differentiating equation (B5) and rearranging give

$$\frac{dT_a}{dx} = \frac{dT_g}{dx} - \frac{d\theta}{dx} \tag{B7}$$

[redacted]

Substituting equations (B2) and (B4) into equation (B7) and rearranging give

$$\frac{d\theta}{dx} + \frac{\theta}{B} = \frac{\pi}{2L}\left(T_{g,1} - T_{g,0}\right) \cos \frac{\pi}{2}\frac{x}{L} \tag{B8}$$

which has the general solution

$$\theta = Ce^{-\frac{x}{B}} + 2\pi LB \frac{\left(T_{g,1} - T_{g,0}\right)}{(\pi B)^2 + 4L^2} \cos \frac{\pi}{2}\frac{x}{L} + (\pi B)^2 \frac{\left(T_{g,1} - T_{g,0}\right)}{(\pi B)^2 + 4L^2} \sin \frac{\pi}{2}\frac{x}{L} \tag{B9}$$

Substituting boundary conditions $\theta = T_{g,0} - T_{a,0}$ when $x = 0$ into (B9), evaluating C, and rearranging give

$$\frac{T_{g,x} - T_{a,x}}{T_{g,1} - T_{g,0}} = \left(\frac{T_{g,0} - T_{a,0}}{T_{g,1} - T_{g,0}} - \frac{2\pi LB}{(\pi B)^2 + 4L^2}\right) e^{-\frac{x}{B}} + \frac{2\pi LB}{(\pi B)^2 + 4L^2} \cos \frac{\pi}{2}\frac{x}{L} + \frac{(\pi B)^2}{(\pi B)^2 + 4L^2} \sin \frac{\pi}{2}\frac{x}{L} \tag{B10}$$

Thus, the cooling-air temperature at any point x is given in terms of the known parameters $\frac{x}{L}$, B, and $\frac{T_{g,0} - T_{a,0}}{T_{g,1} - T_{g,0}}$ and the dependent parameter $\frac{T_{g,x} - T_{a,x}}{T_{g,1} - T_{g,0}}$ in which $T_{g,x}$ is found from equation (B1).

[redacted]

DECLASSIFIED

APPENDIX C

SAMPLE PROBLEM

It is desired to calculate the average inside wall temperature at station F for afterburner configuration A of this report. The following conditions are given:

Burner inlet total temperature, $T_{g,0}$, $^{\circ}R$	1633
Exhaust-gas total temperature, $T_{g,1}$, $^{\circ}R$	3425
Inlet cooling-air temperature, $T_{a,0}$, $^{\circ}R$	771
Cooling-air flow, W_a, lb/sec	3.15
Combustion-gas flow, W_g, lb/sec	22.3
Fraction of combustion-chamber length, x/L	0.651

The cooling-air temperature $T_{a,F}$ is found from figures 13 and 14. From figure 13, $(T_{a,F})_{0.12} = 977^{\circ}$ R, corresponding to $T_{a,0} = 771^{\circ}$ R and $T_{g,1} = 3425^{\circ}$ R. The mass-flow ratio is

$$\frac{W_a}{W_g} = \frac{3.15}{22.3} = 0.1412$$

Therefore, $f = 0.987$ from figure 14, corresponding to $W_a/W_g = 0.1412$ and $T_{a,0} = 771^{\circ}$ R. The cooling air temperature at station F is $T_{a,F} = f(T_{a,F})_{0.12} = 0.987 \times 977 = 965^{\circ}$ R.

The combustion-gas temperature $T_{g,F}$ is obtained from equation (11)

$$\frac{T_{g,F} - T_{g,0}}{T_{g,1} - T_{g,0}} = \sin \frac{\pi}{2} \frac{x_F}{L}$$

which, upon rearranging, gives

$$T_{g,F} = (T_{g,1} - T_{g,0}) \sin \frac{\pi}{2} \frac{x_F}{L} + T_{g,0}$$

$$= (3425 - 1633)\ 0.853 + 1633 = 3162^{\circ} \text{ R}$$

[redacted]

03712A039

and

$$\frac{T_{a,F}}{T_{g,F}} = \frac{965}{3162} = 0.305$$

Substituting into equation (12) gives

$$\frac{T_{g,F} - T_{w,F}}{T_{w,F} - T_{a,F}} = 30(0.305)^{0.73}\ (0.1412)^{0.80}$$

$$= 2.64$$

and rearranging gives

$$T_{w,F} = \frac{T_{g,F} + 2.64\ T_{a,F}}{3.64} = \frac{3425 + 2.64 \times 965}{3.64}$$

$$= 1641^{\circ}\ R$$

REFERENCES

1. Koffel, William K., and Kaufman, Harold R.: Cooling Characteristics of an Experimental Tail-Pipe Burner with an Annular Cooling-Air Passage. NACA RM E51K23, 1952.

2. Koffel, William K., and Kaufman, Harold R.: Investigation of Heat-Transfer Coefficients in an Afterburner. NACA RM E52D11, 1952.

3. McAdams, William H.: Heat Transmission. McGraw-Hill Book Co., Inc., 2d ed., 1942, pp. 170-172.

4. The Staff of the Ames 1- by 3-Foot Supersonic Wind-Tunnel Section: Notes and Tables for Use in the Analysis of Supersonic Flow. NACA TN 1428, 1947.

5. Pinkel, I. Irving: Determination of Ram-Jet Combustion-Chamber Temperatures by Means of Total-Pressure Surveys. NACA TN 2526, 1952.

6. Boelter, L. M. K., Martinelli, R. C., Romie, F. E., and Marrin, E. H.: An Investigation of Aircraft Heaters. XVIII - A Design Manual for Exhaust Gas and Air Heat Exchangers. NACA ARR 5A06, 1945, pp. 27-32.

[redacted]

DECLASSIFIED

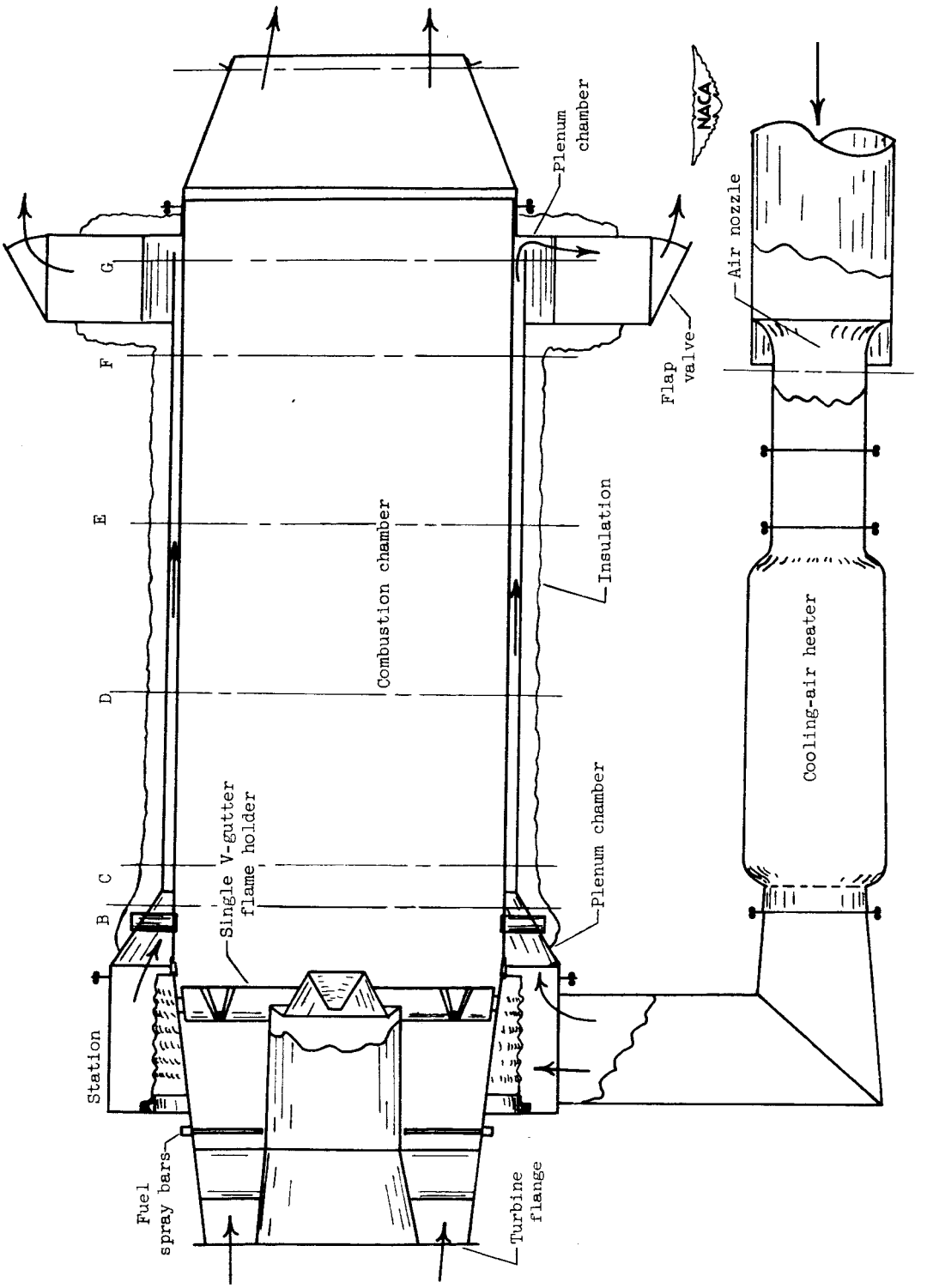

Figure 1. - Schematic diagram of afterburner.

[redacted]

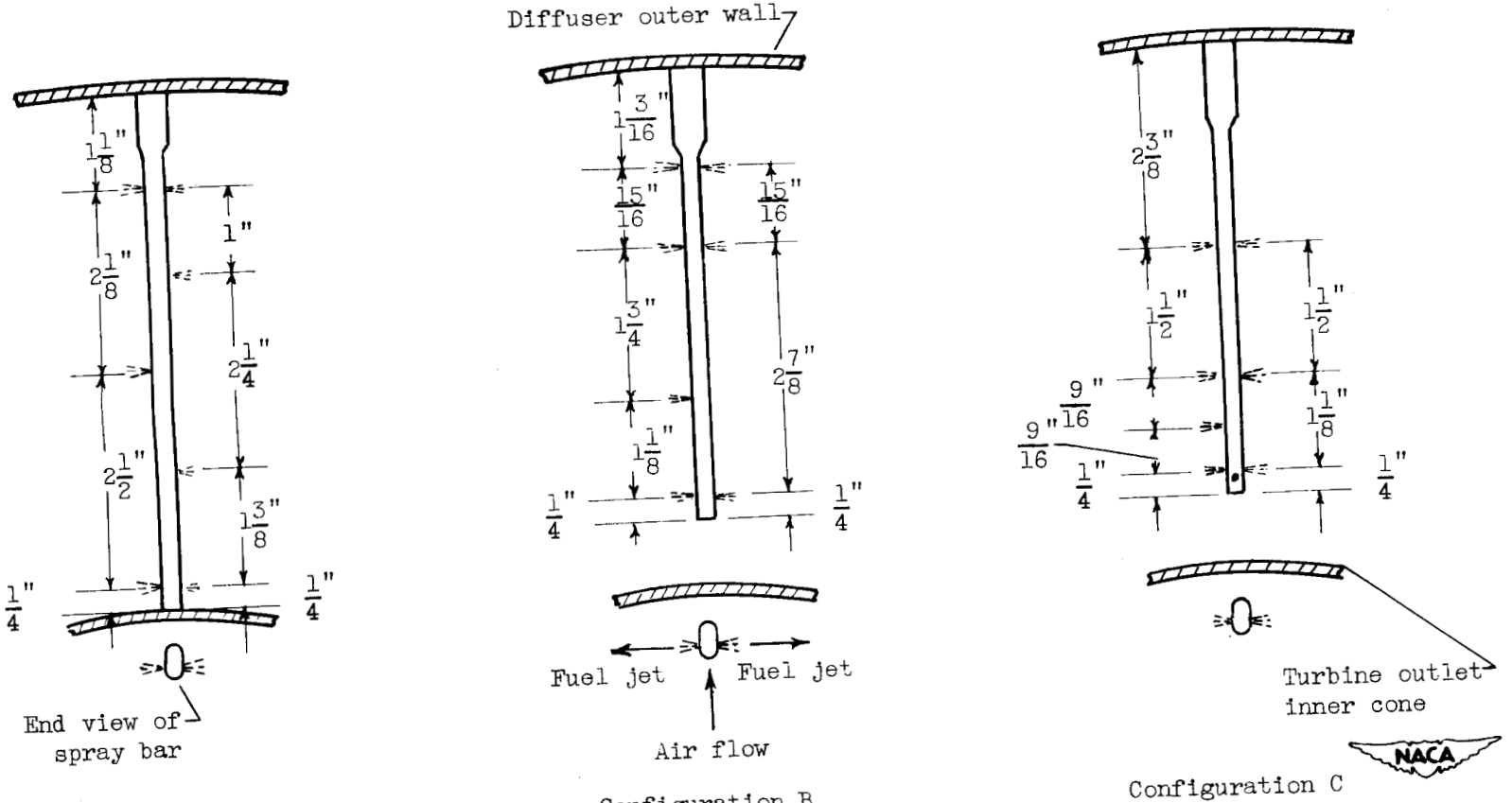

Figure 2. - Downstream view of turbine-outlet annulus showing fuel spray bars for configurations A, B, and C. Diameter of fuel jets, 0.020 inch.

DECLASSIFIED

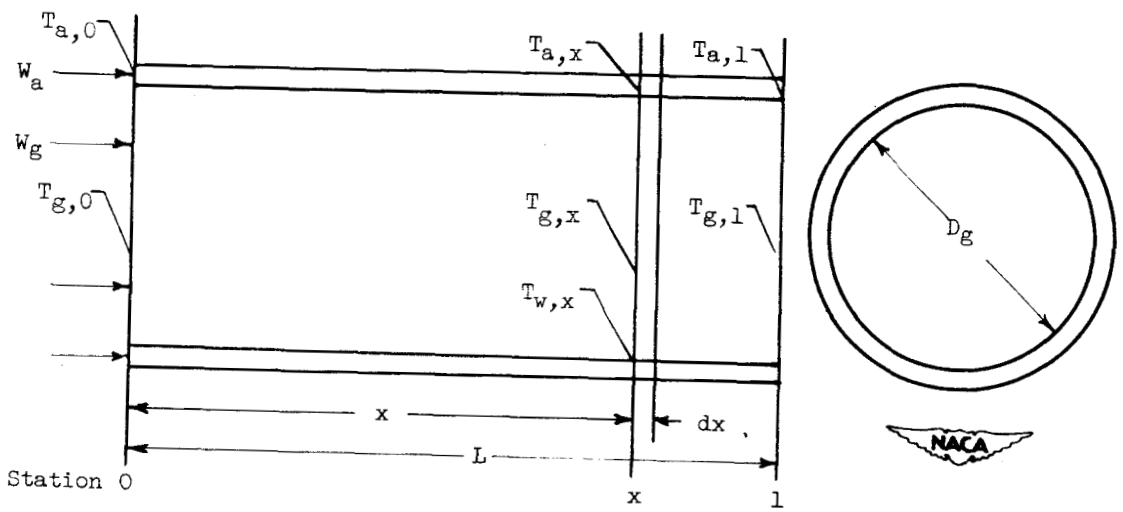

Figure 3. - Schematic diagram of idealized heat exchanger.

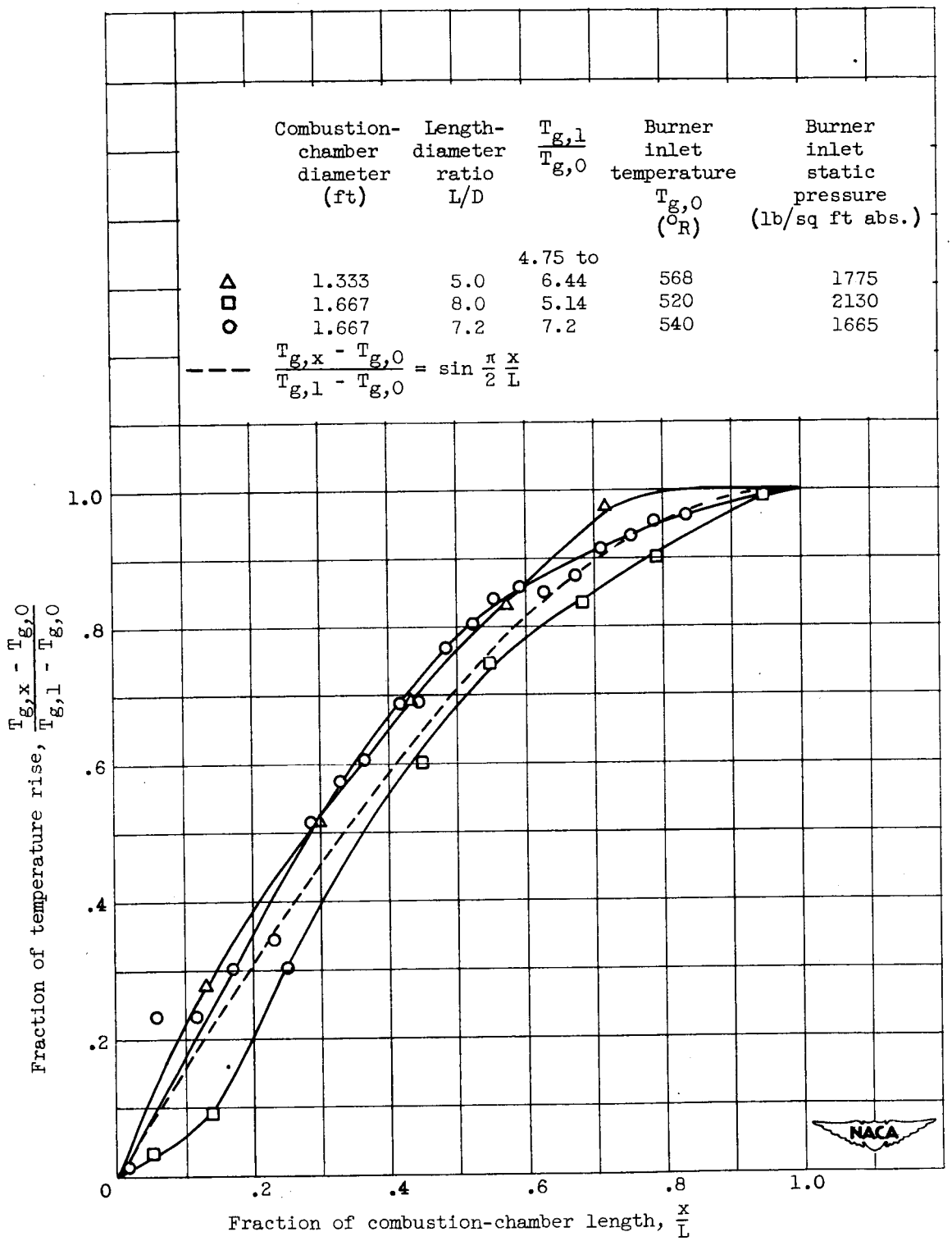

Figure 4. - Generalized longitudinal profile of combustion-gas total temperature for several ram-jet combustion chambers.

UNCLASSIFIED

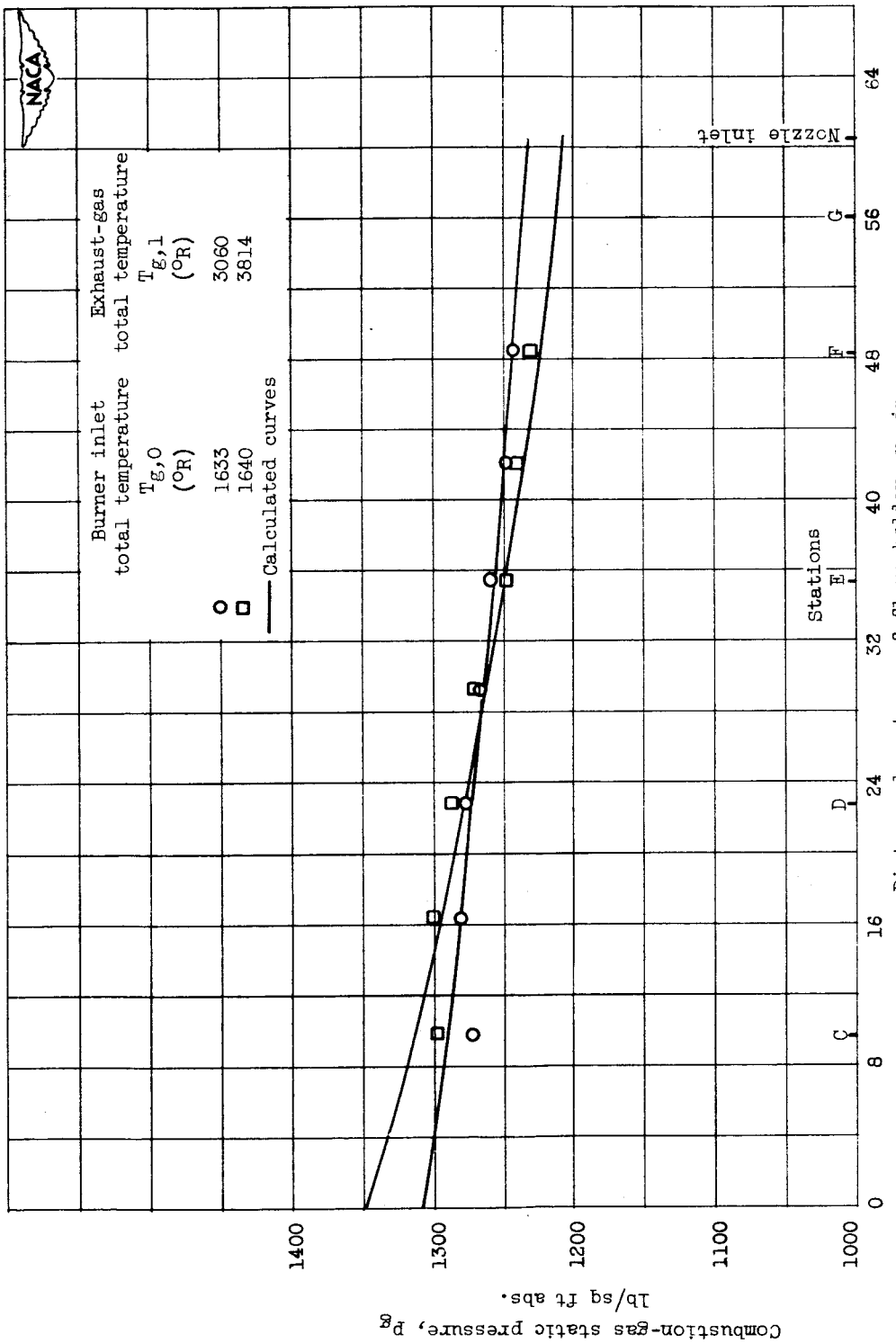

Figure 5. - Comparison of experimental static-pressure distribution with calculated pressure distribution based on equation $\frac{T_{g,x} - T_{g,0}}{T_{g,1} - T_{g,0}} = \sin \frac{\pi}{2} \frac{x}{L}$ for L = 74.5 inches.

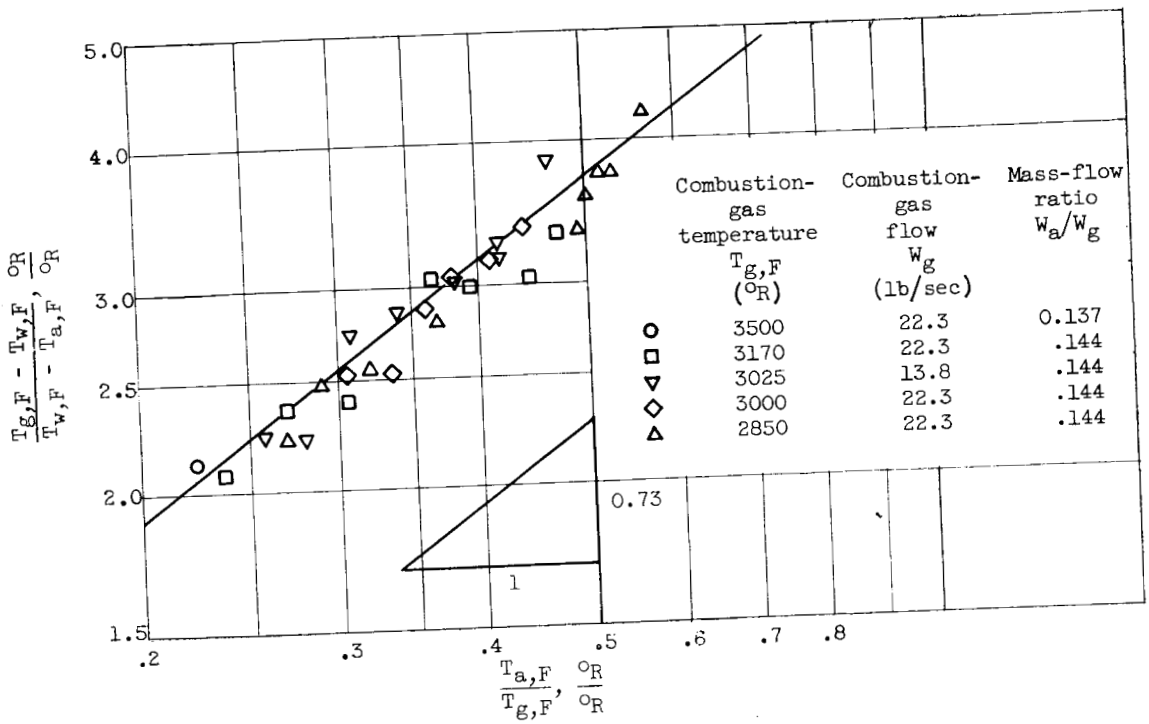

(a) Determination of p.

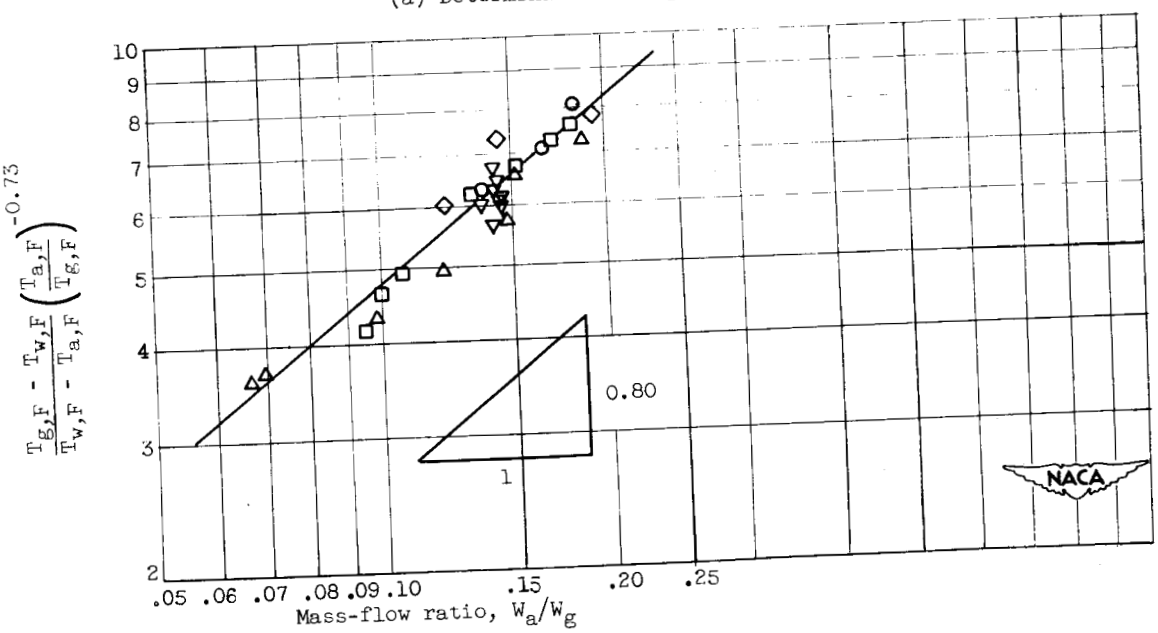

(b) Determination of m.

Figure 6. - Determination of empirical constants in equation (10). Configuration A at station F.

DECLASSIFIED

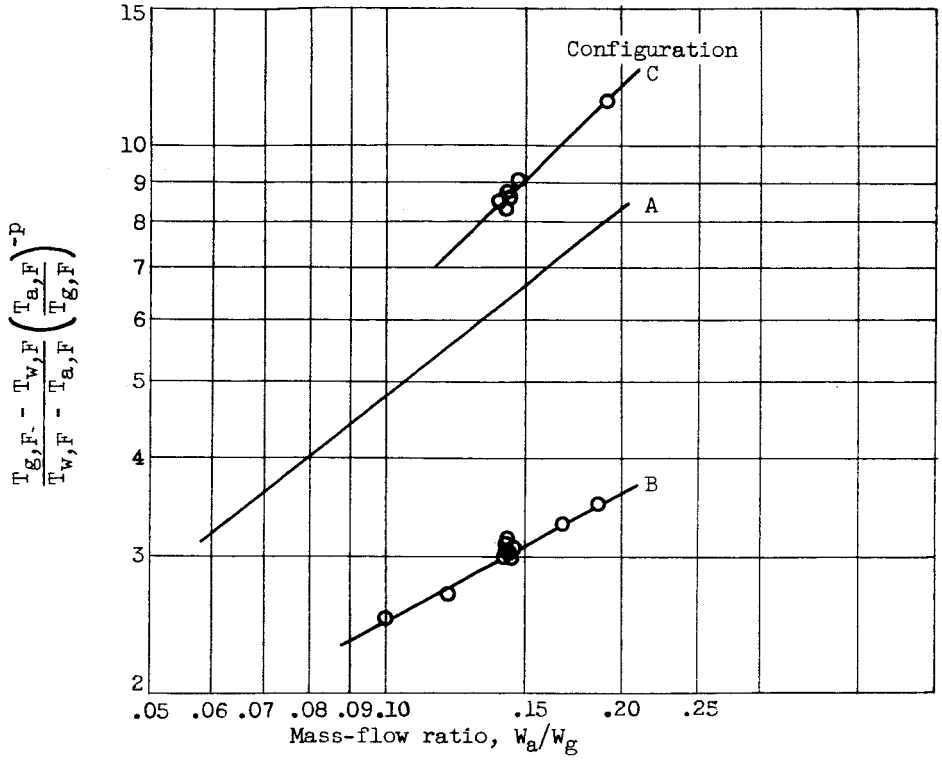

Figure 7. - Graphical comparison of cooling correlations for three radial distributions of afterburner fuel at station F.

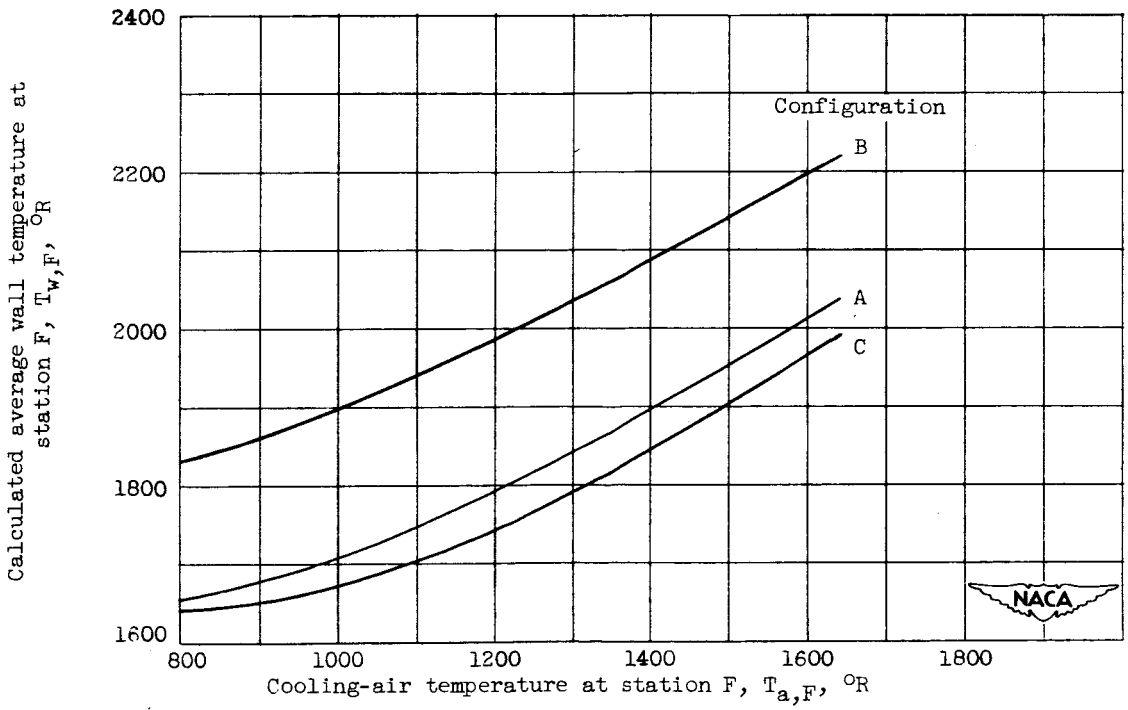

Figure 8. - Comparison of calculated average wall temperature at station F for three configurations. Combustion-gas temperature, 3500° R; mass-flow ratio, 0.143.

[redacted]

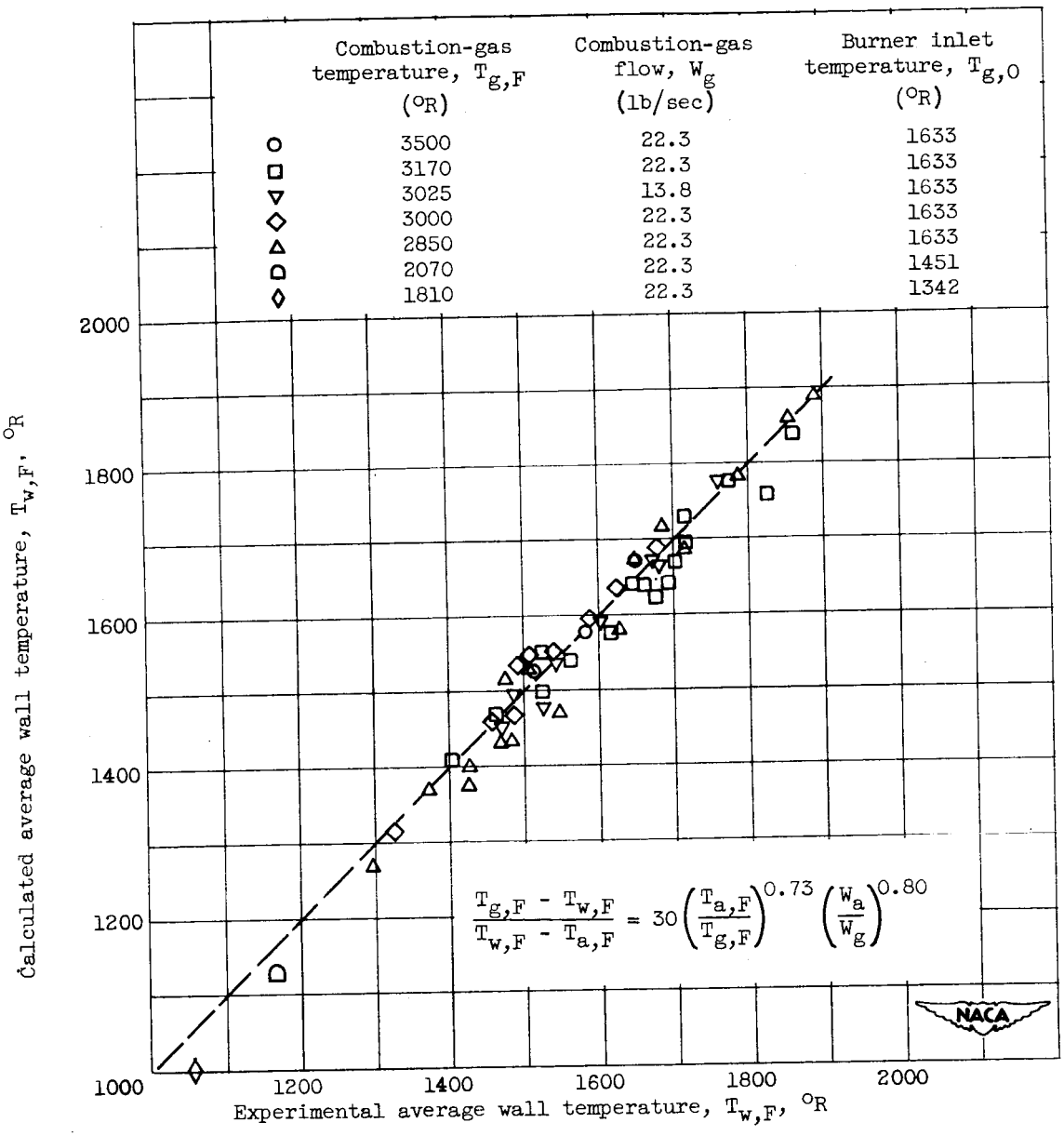

(a) Experimental cooling-air temperature, $T_{a,F}$.

Figure 9. - Comparison of calculated wall temperature with experimental wall temperature at station F for configuration A.

UNCLASSIFIED

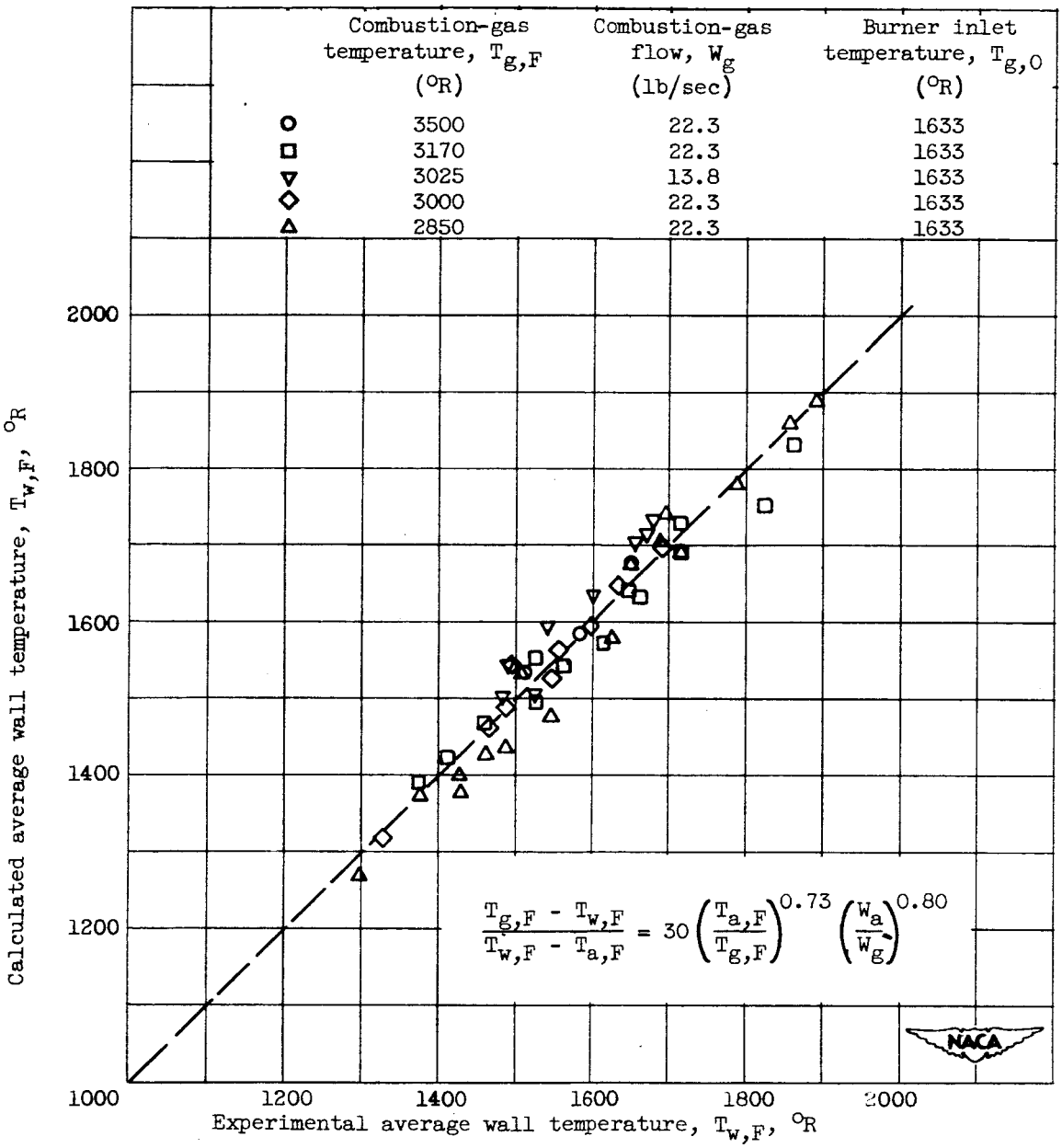

(b) Cooling-air temperature $T_{a,F}$ from figures 13 and 14.

Figure 9. - Concluded. Comparison of calculated wall temperature with experimental wall temperature at station F for configuration A.

[redacted]

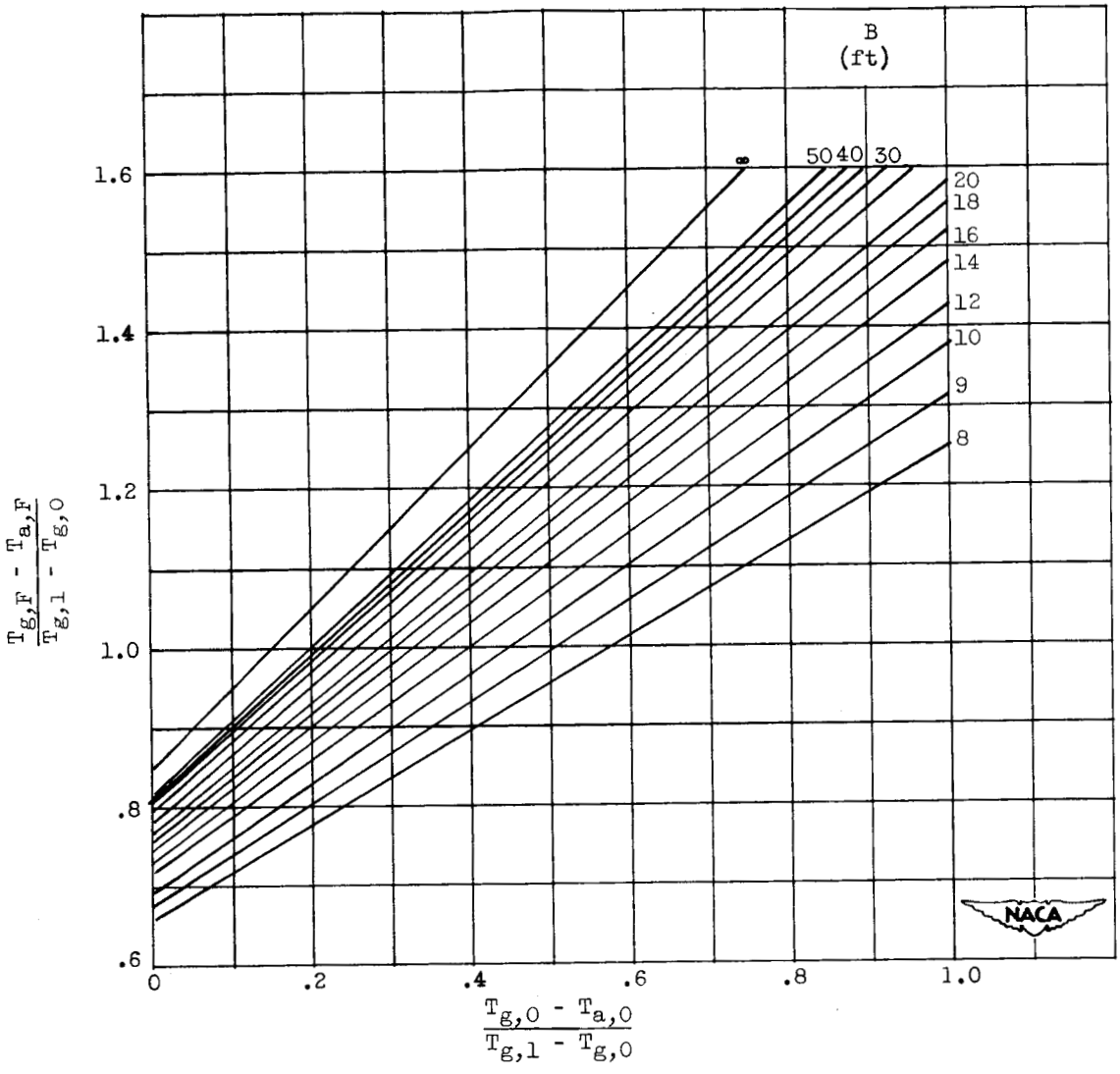

Figure 10. - Performance characteristics of idealized heat exchanger having constant over-all heat-transfer coefficient. Station F (x/L = 0.651).

$$\frac{T_{g,x} - T_{a,x}}{T_{g,1} - T_{g,0}} = \left(\frac{T_{g,0} - T_{a,0}}{T_{g,1} - T_{g,0}} - \frac{2\pi LB}{(\pi B)^2 + (2L)^2} \right) e^{-x/B} + \frac{2\pi LB}{(\pi B)^2 + (2L)^2} \cos \frac{\pi}{2} \frac{x}{L} + \frac{(\pi B)^2}{(\pi B)^2 + (2L)^2} \sin \frac{\pi}{2} \frac{x}{L}$$

where $B = \frac{3600\ W_a c_{p,a}}{U \pi D_g}$ and $T_{g,x}$ is defined by $\frac{T_{g,x} - T_{g,0}}{T_{g,1} - T_{g,0}} = \sin \frac{\pi}{2} \frac{x}{L}$

DECLASSIFIED

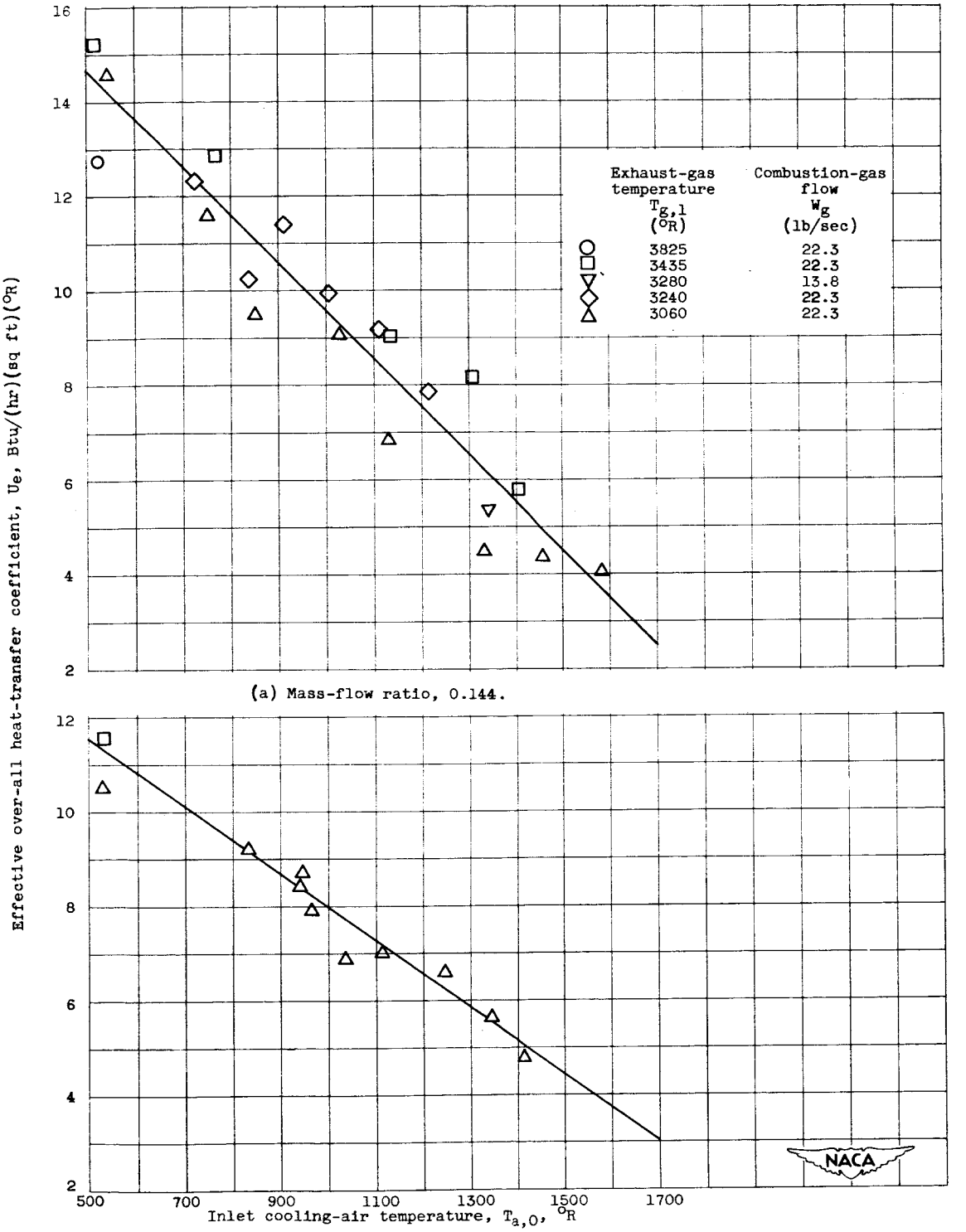

Figure 11. - Variation of effective over-all heat-transfer coefficient with inlet cooling-air temperature. Burner inlet temperature, 1633° R.

[redacted]

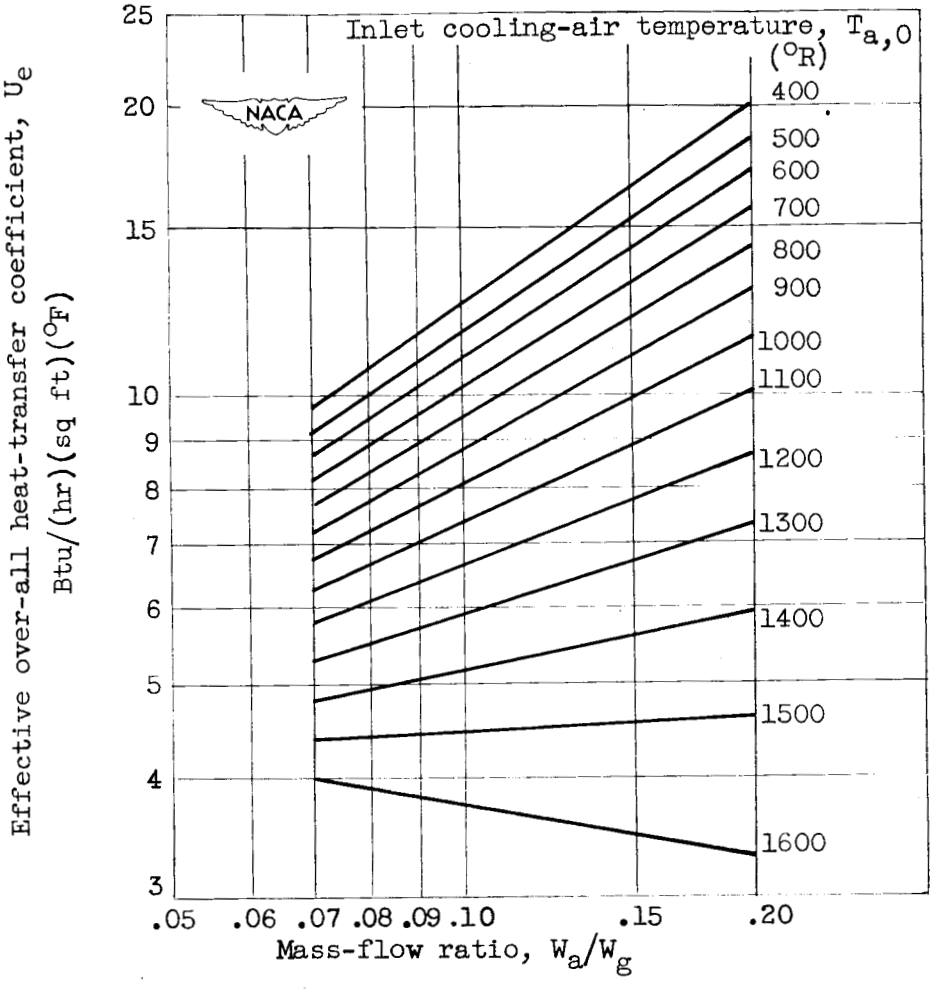

Figure 12. - Variation of effective over-all heat-transfer coefficient with mass-flow ratio of cooling air to combustion gas. Combustion-gas flow, 22.3 pounds per second.

DECLASSIFIED

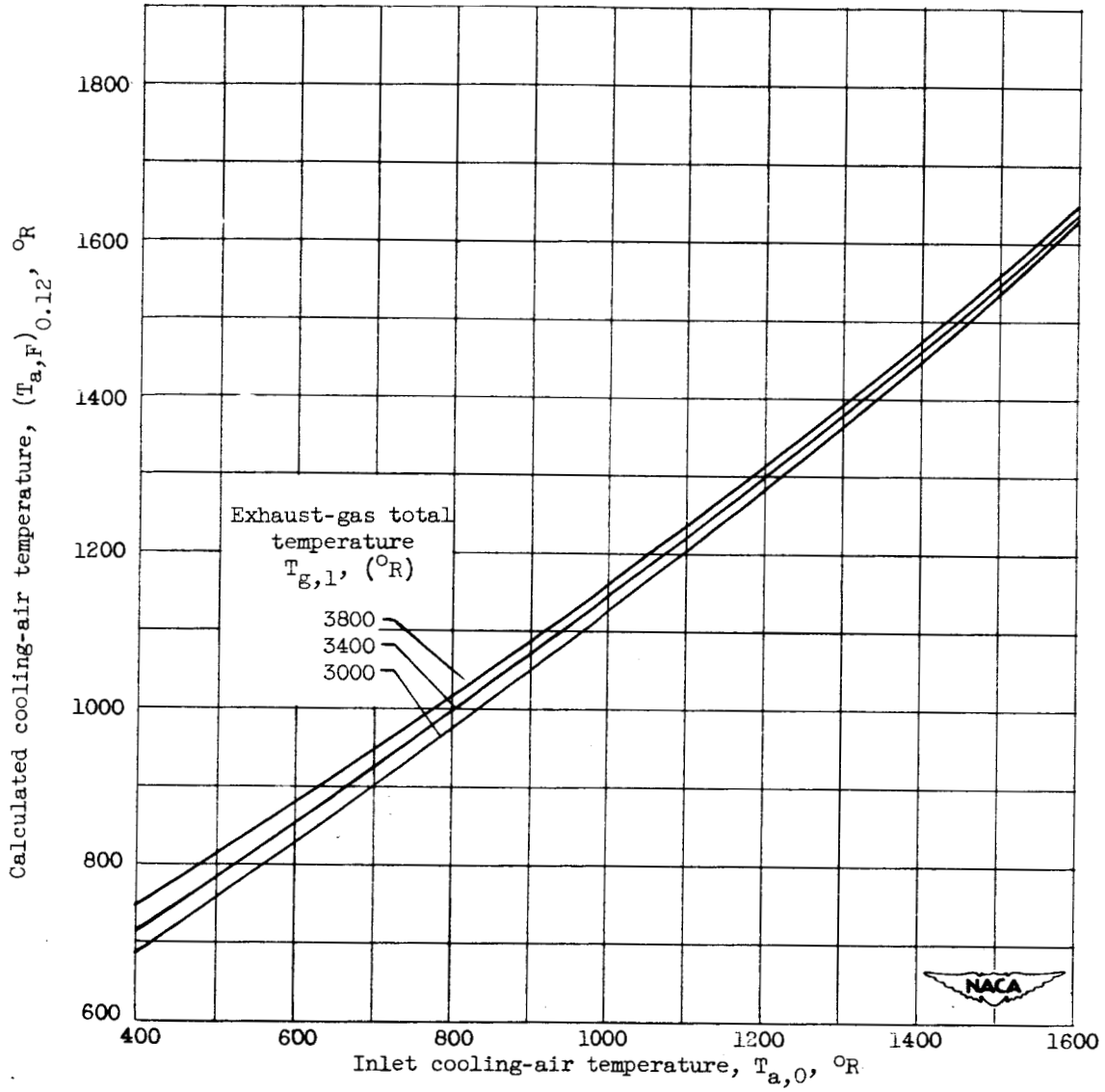

Figure 13. - Variation of calculated cooling-air temperature at station F with inlet cooling-air temperature at mass-flow ratio of 0.12. Burner inlet temperature, 1633° R.

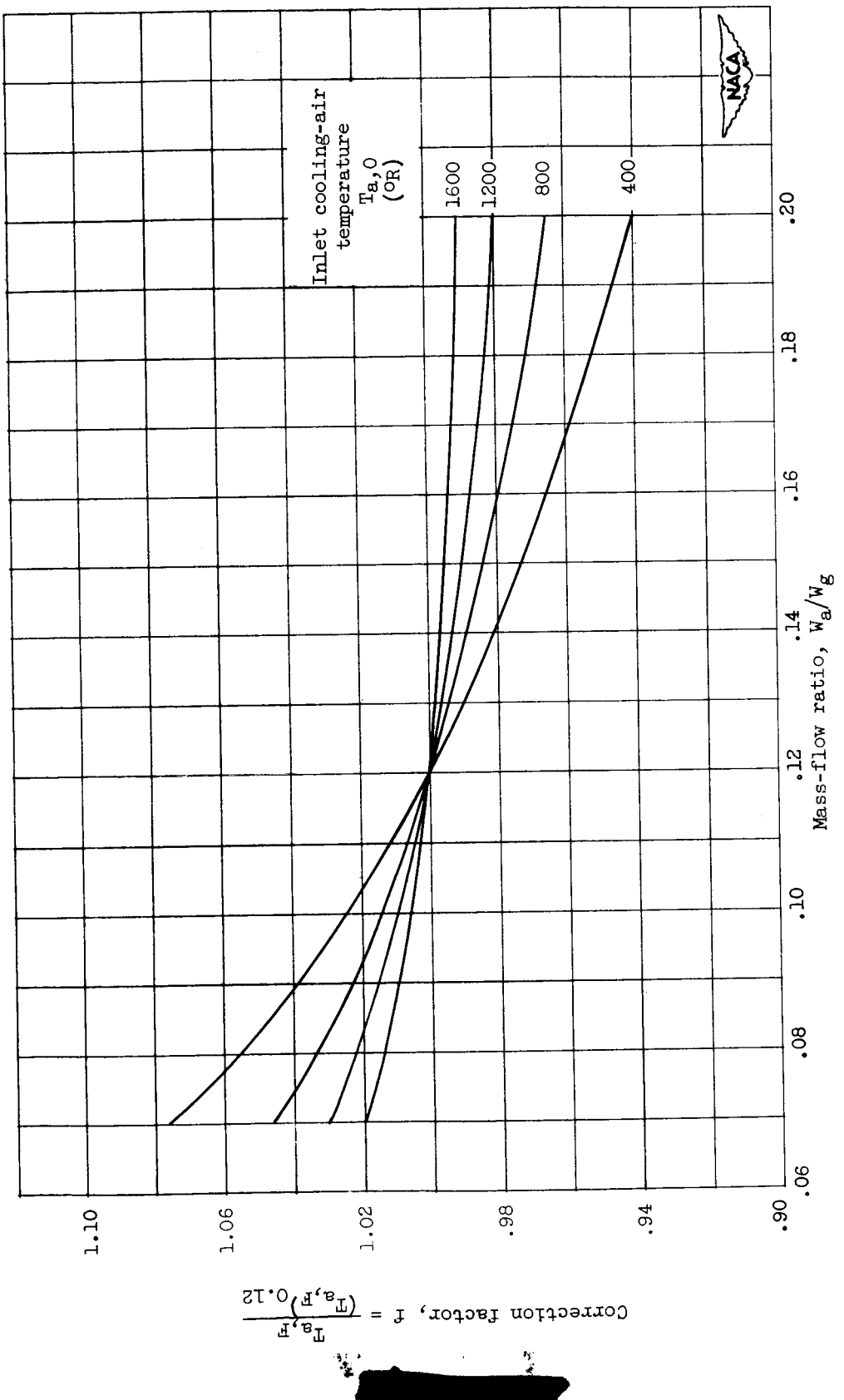

Figure 14. - Correction factor for cooling-air temperature at station F against mass-flow ratio for exhaust-gas temperatures from 3000° to 3800° R. Burner inlet temperature, 1633° R.